



Supplement of

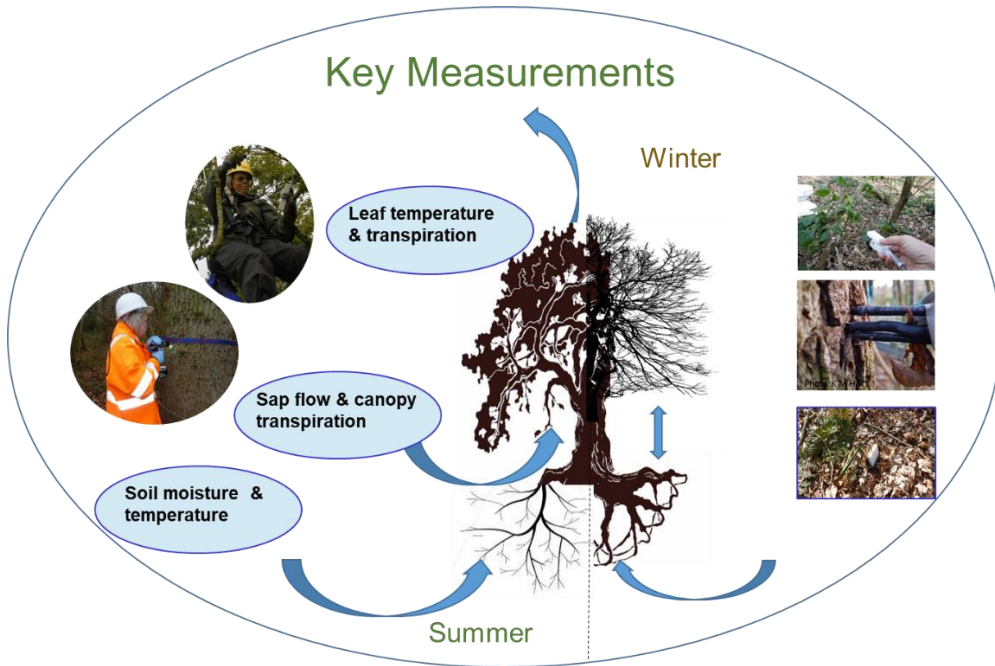
Water usage of old-growth oak at elevated CO₂ in the FACE (Free-Air CO₂ Enrichment) of climate change

Susan E. Quick et al.

Correspondence to: A. Robert MacKenzie (a.r.mackenzie@bham.ac.uk)

The copyright of individual parts of the supplement might differ from the article licence.

Supplementary information.
Section 2.2



5 Figure S1: Key plant hydraulic related measurements.

Tree ID	Array No.	Treatment	Install & Measure date	Initial Circumference (m)	Initial Average R _b at probeset (m)	2022 Circumference (m)	2022 Average R _b at probeset (m)	Average probeset height (m)
8467	1	eCO ₂	13/07/2017	1.640	<u>0.261</u>	1.656	<u>0.264</u>	1.13
8468	1	eCO ₂	13/07/2017	1.720	0.274	1.734	0.276	1.2
8673	2	aCO ₂	28/08/2018	2.360	0.376	2.372	0.378	1.26
8749	2	aCO ₂	28/08/2018	2.600	0.414	2.636	0.420	1.2
8351	3	aCO ₂	20/07/2017	1.710	0.272	1.726	0.275	1.19
9301	3	aCO ₂	20/07/2017	2.560	0.407	2.621	0.417	1.13
6621	4	eCO ₂	28/08/2018	2.350	0.374	2.372	0.378	1.3
6632	4	eCO ₂	05/09/2018	2.270	0.361	2.288	0.364	1.28
6382	5	aCO ₂	18/07/2018	2.210	0.352	2.220	0.353	1.3
6406	5	aCO ₂	18/07/2018	2.890	0.460	2.864	0.456	1.28
3755	6	eCO ₂	17/07/2018	2.260	0.360	2.278	0.363	1.23
5846	6	eCO ₂	17/07/2018	2.920	0.465*	2.968	0.472*	1.3
6027	7	none/ <i>Ghost</i>	21/07/2017	2.050	0.326	2.104	0.335	1.29
6021	7	none/ <i>Ghost</i>	21/07/2017	2.620	0.417	2.644	0.421	1.23
3642	8	none/ <i>Ghost</i>	24/07/2017	1.720	0.274	1.790	0.285	1.24
3634	8	none/ <i>Ghost</i>	24/07/2017	2.690	0.428	2.718	0.433	1.28
7476	9	none/ <i>Ghost</i>	05/01/2017	2.160	0.344	2.202	0.350	1.3
7331	9	none/ <i>Ghost</i>	05/07/2017	2.500	0.398	2.556	0.407	1.25

Table S1: Tree identification, array number, treatment type, species and installation/ measurement dates along with circumference and diameter at probeset insertion point height for target oak trees at start and in 2022. Underlined R_b values are smallest (initial & 2022). Largest R_b is marked with an asterix. See also Table S3 for summary data by treatment type.

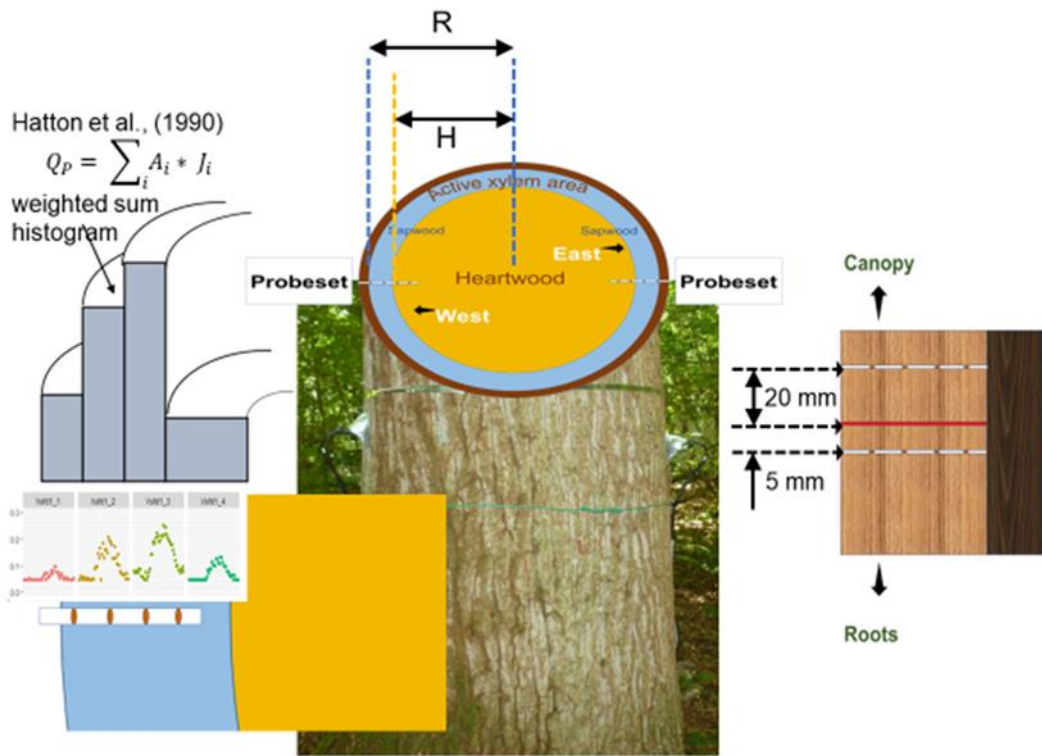


Figure S2: Showing sap probeset layout, spacing dimensions between probes and indicative illustration of Hatton et al., (1990) weighted sum histogram, where R (m) is the radius to the cambium and H (m) is the heartwood estimated radius, both at the probeset insertion height. All equations and variables also defined in Tables A1 and A2. Graphical insert is Fig. C1(b) in main text.

15

Section 2.2 to 2.7

Description	Make	Model	Position	Parameter	Parameter symbol	Where	Units	Sampling rate	Logger rate
Shallow soil moisture. 12 cm water content reflectometry (WCR)	Campbell Scientific [Logan, USA]	CS655 ±3% v/v for typical soils	Inserted from ground level	Volumetric water content (VWC) + Surface soil temperature	<i>n/a</i>	Various all Arrays	% °C		At least every 30 mins
Tipping bucket gauges Half-hourly totals were compiled	Campbell Scientific	ARG100	Ground level	throughfall precipitation - accumulative	P_{fs}	all Arrays	mm		30 mins
FACE hemispherical solar radiation	Hukseflux pyranometer	LP02-03	Top canopy (c25 m)	Total Solar Radiation (Av)	TG	A 1-6	Watt m ⁻²	10 secs	Every hour
FACE temperature sensor (thermistor)	Campbell Scientific	T107	Top canopy (c20 m)	Air Temp (Av)	T_a	A 1-6	°C	10 secs	Every hour
Met tower precipitation	Texas Electronics (Dallas; Texas)	TR-525M	2 m above ground	Precipitation - accumulative	P	Met Towers	mm		15 minutes
Microcores	fCMC, Italy on behalf of UNIVERSITA' di PADOVA	Trephor (Rossi et al., n.d.)	At sap probe insertion height	15mm and 25 mm long, 2mm diameter cores for wood characteristics	<i>n/a</i>				

Table S2: Soil, precipitation, FACE and Met tower instrumentation. Also microcorer equipment type.

Section 2.7

2022	Tree	GH	Tree	aCO ₂	Tree	eCO ₂
	6027	2.104	8673	2.372	8467	1.656
	6021	2.644	8749	2.636	8468	1.734
	3642	1.79	8351	1.726	6621	2.372
	3634	2.718	9301	2.621	6632	2.288
	7476	2.202	6382	2.22	3755	2.278
	7331	2.556	6406	2.864	5846	2.968
	mean circumference	2.34		2.41		2.22

sm	3642	1.79	sm	8351	1.726	sm	8467	1.656
med	7476	2.202	med	8673	2.372	med	6632	2.288
lg	3634	2.718	lg	6406	2.864	lg	5846	2.968

20 **Table S3: To show tree stem circumference measures in 2022 for all trees. Also mean circumference (metres) and sizes of smallest (sm), largest (lg) and medium (med) sized trees in each treatment category.**

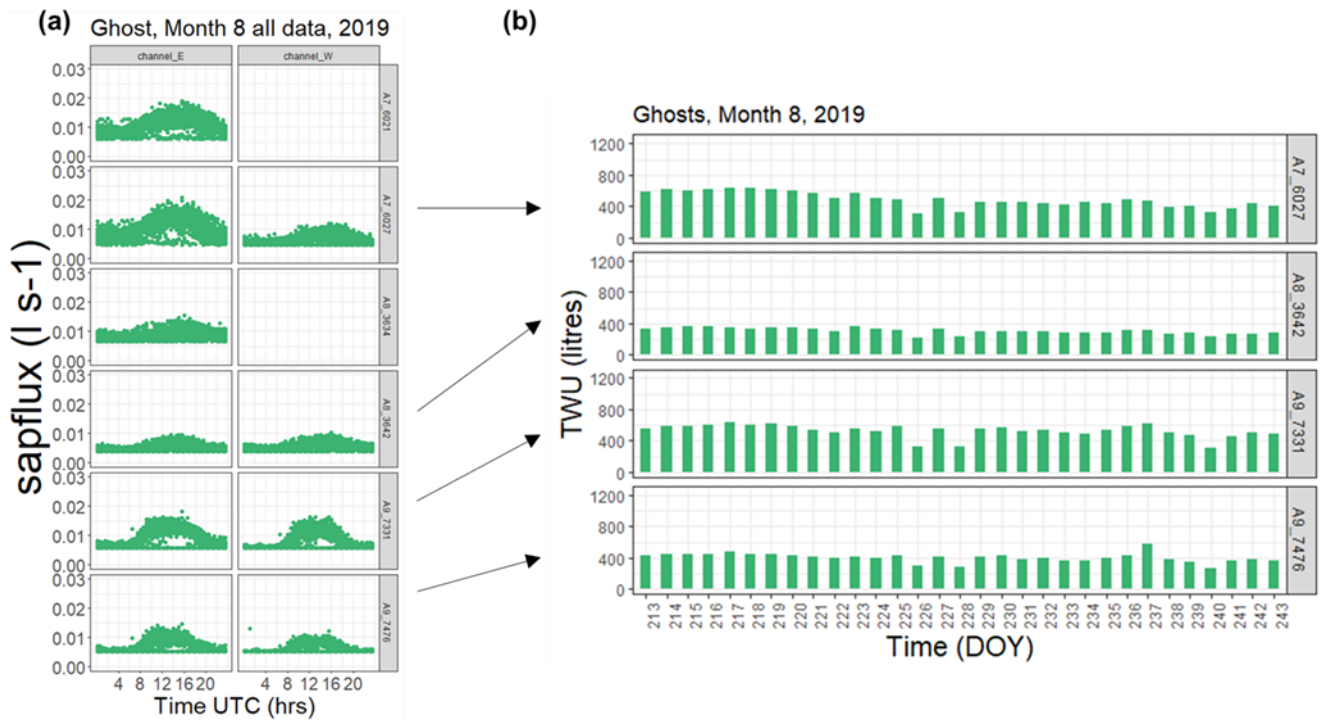
Notes to Table S3.

All oak trees were of similar height (circa 25 m). Tree stem circumference at insertion height of probes was measured at installation (from 2017 onwards), using a standard tape measure, and checked manually in subsequent winters (Jan 2020-Feb 2022). The range and mean-per-treatment values of bark circumference (metres) for all target trees are tabulated and are summarised as follows: *Ghost* mean 2.34 m, range 1.79–2.72 m; aCO₂ mean 2.41 m (3% larger than the *Ghost* control mean), range 1.73–2.86 m; eCO₂ mean 2.22 m (5% smaller than the *Ghost* control mean), range 1.66–2.97 m.

Section 2.8

Parameter	Author	Reported value	Conversion factor	Metric equivalent	Tree size
Sap flux (density) maximum	Tatarinov (2005)	0.1 kg cm ⁻² h ⁻¹	10 ⁴ / 3600	2.7778 x 10 ⁻¹ Kg m ⁻² s ⁻¹ [litres m ⁻² s ⁻¹]	Dbh>30cm, Height=29m
Sapflux max hourly (mean of 2x trees)	Sanchez-Perez (2008) HP	The hourly Maximum (total) fluxes were [30 litres h ⁻¹].		The hourly maximum fluxes were [30 litres h ⁻¹]. [July circa 380 (litres tree ⁻¹ day ⁻¹)] see below	Dbh=83cm Height=22
Total daily sapflux (summer max)	Čermák et al (1992) ref in Tatarinov (2005)*	200 kg tree ⁻¹ h ⁻¹		200 kg tree ⁻¹ h ⁻¹ [circa 1600 (kg tree ⁻¹ day ⁻¹)]	Dbh=30cm Height=29m
Total daily sapflux mean	Sanchez-Perez (2008) HP		N/A	[385 +/-41 l tree ⁻¹ day ⁻¹ July 1996]	Dbh=83cm Height=22
Total daily sapflux max *Q.suber	David (2013)	250 (kg tree ⁻¹ day ⁻¹)		250 (kg tree ⁻¹ day ⁻¹)	
Breast height Sap flux area (typical)	(Čermák et al (1992) & as quoted/Implied Tatarinov (2005)	2000 cm +2	10 ⁻⁴	2.0 x 10 ⁻¹ (m +2)	

30 Table S4: Comparison of sap parameters with other studies of oak.



35 **Figure S 3: Example *Ghost* Array xylem sap responses in August 2019. (a) diel (24hour) tree sap flux for all days in August 2019 are superimposed. E (left) and W (right) facing probesets for six *Ghost* trees show circumferential imbalance in xylem flux. All data for the individual month is superimposed across time-of-day sampling (hours, UTC). Frequency of sampling is every 0.5 hrs. Faulty probeset positions are shown blank. (b) Example of accumulative daily diurnal water usage (*TWU*) per tree totalled for E and W facing probesets across month 8 2019 for four *Ghost* trees having both E and W probesets functioning with the other two *Ghost* trees omitted due to faulty probesets. Time is day-of-year (DOY).**

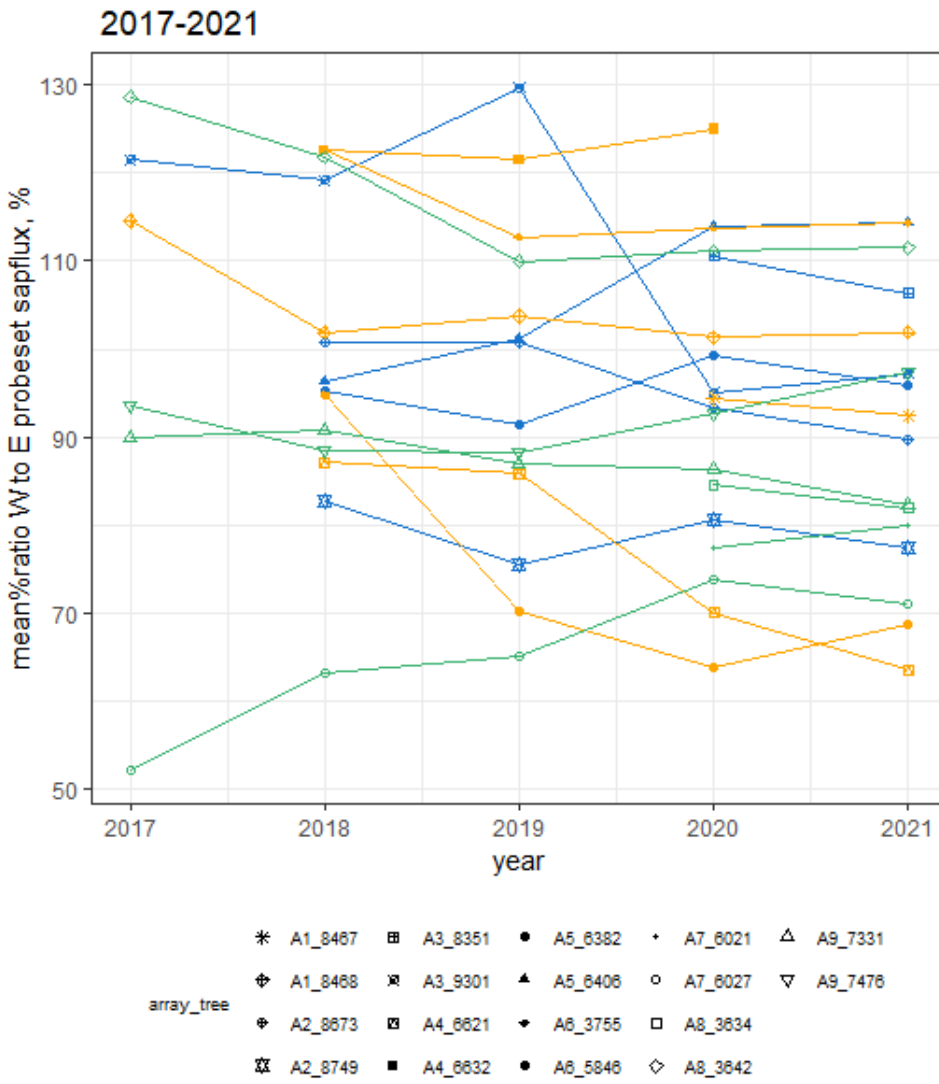
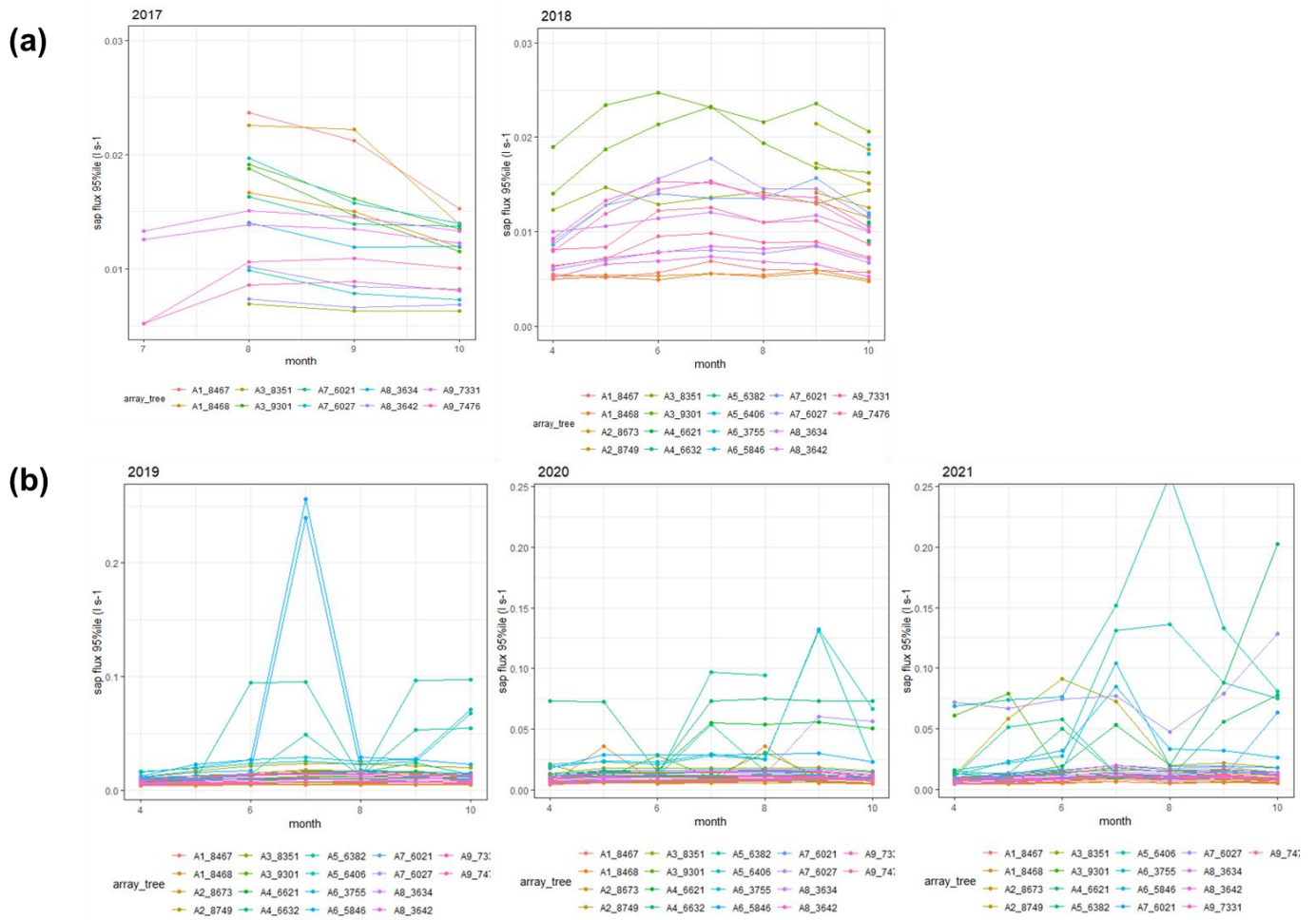


Figure S4: Imbalance of median sap flux values for each probeset by tree. Tree sapflux data for W- facing probeset as a percentage of E-facing sapflux data, averaged for each year of two probeset operation. Points are derived from means of monthly median probeset sapflux values for each tree. Note 2017 is only a partial year.



45 **Figure S5:** In years 2017 to 2021, summary monthly treatment season 95%ile sap flux ($l s^{-1}$) for each functional probeset all trees are shown. Colours represent individual trees and are also labelled with Array number (Ax). A1, A4, A6 are eCO_2 trees, A3, A2, A5 are aCO_2 trees, A7, A8, A9 are *Ghost* trees. (a) years 2017 and 2018, scaled to show a maximum of $0.03 l s^{-1}$. (b) years 2019, 2020 and 2021, scaled to show a maximum of $0.25 l s^{-1}$.

Section 3.2

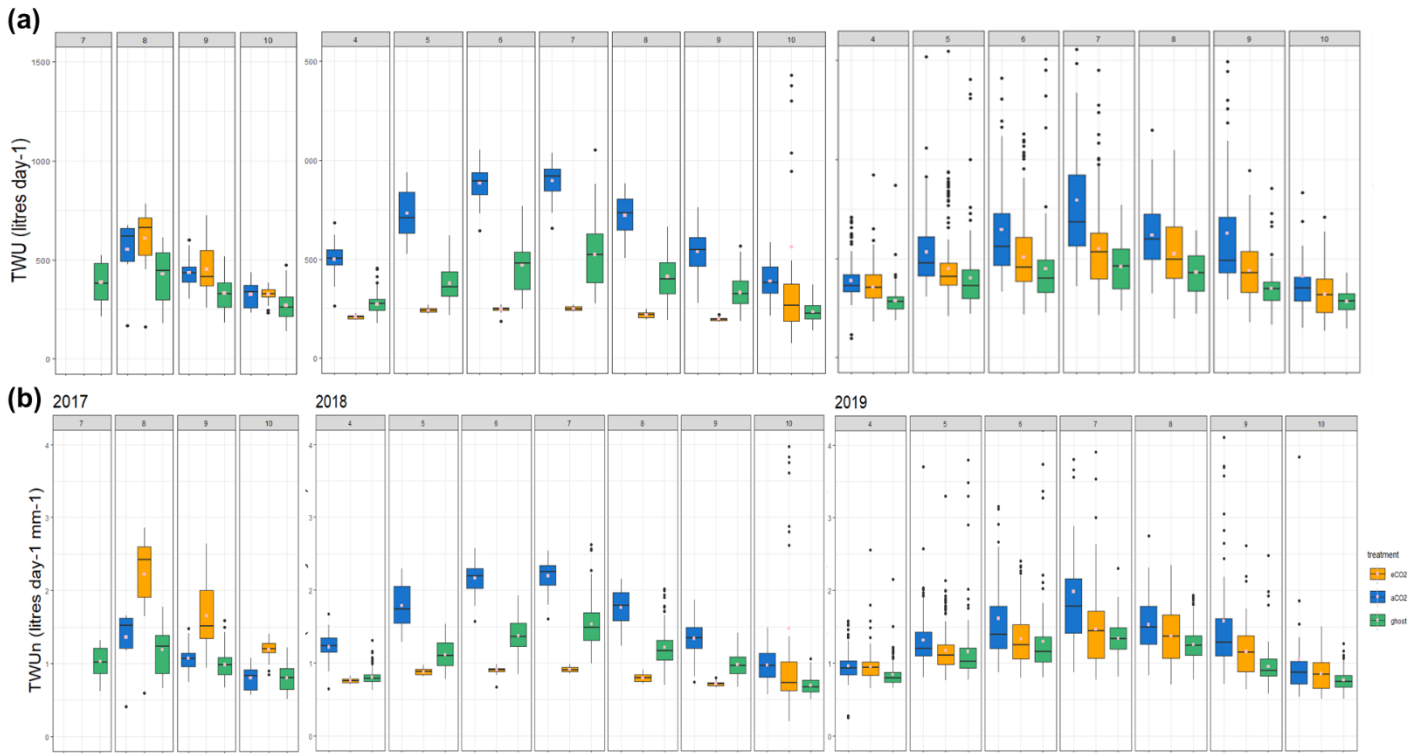
	Slope (litres $d^{-1} mm^{-1}$)	SE	intercept	t	df	p
aCO₂	3.86	1.25	-775	3.09	16	p<0.01
eCO₂	3.55	0.31	-691	11.53	15	p<0.001
Ghost	1.20	0.47	75.4	2.54	21	p<0.05

50 **Table S5:** Linear regression model parameters for oak mean TWU (\overline{TWU} , litres d^{-1}) across a month (here July) versus bark radius (m) at insertion point. In this table slope, litres per day per millimetre bark radius, is calculated. Data from 2, 6, 12, 18 or 17 trees for years 2017, 2018, 2019, 2020 & 2021 which each have two probesets (E and W facing) fully operational across the month of interest are modelled by treatment for all years combined. July typically exhibits maximum mean TWU (\overline{TWU}) across summer months in control arrays. See also Notes to Table S3 re relative size ranges of trees in the three treatment types.

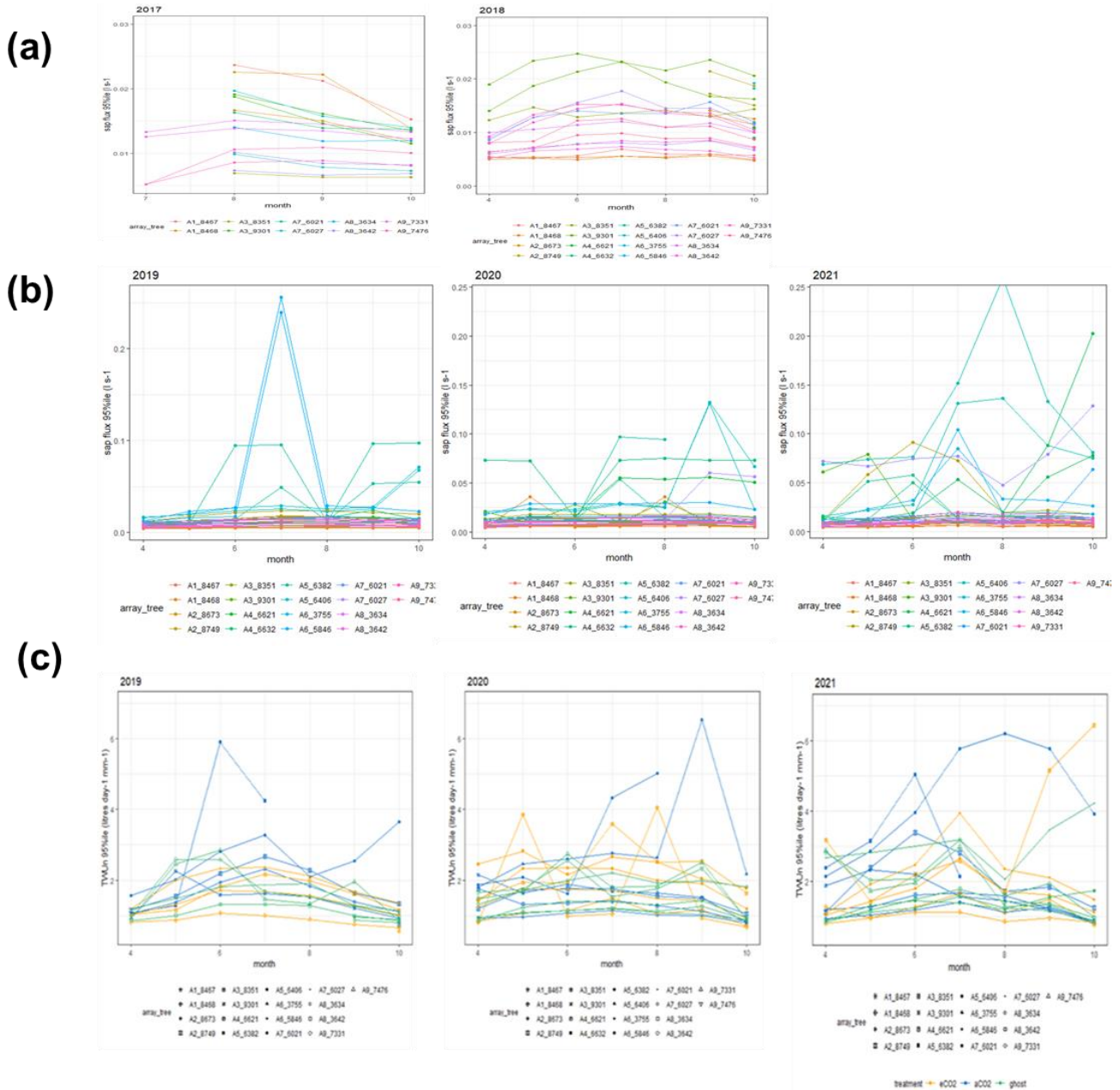
Tree_ID	Array	year	SprdAvdia	TotSpread_dia	CanopyArea	treatment	barkradius	FirstLast
8467	1	2017	9.695	10.217	81.986	eCO2	0.26	First
8467	1	2022	8.377	8.904	62.264	eCO2	0.26	Last
8468	1	2017	9.545	10.092	79.999	eCO2	0.27	First
8468	1	2022	8.92	9.472	70.464	eCO2	0.28	Last
8673	2	2017	15.175	15.926	199.212	aCO2	0.38	First
8673	2	2022	11.448	12.203	116.963	aCO2	0.38	Last
8749	2	2017	12.48	13.308	139.088	aCO2	0.41	First
8749	2	2022	12.947	13.786	149.262	aCO2	0.42	Last
8351	3	2017	13.925	14.469	164.432	aCO2	0.27	First
8351	3	2022	12.398	12.948	131.667	aCO2	0.28	Last
9301	3	2017	16.375	17.19	232.079	aCO2	0.41	First
9301	3	2022	16.083	16.918	224.786	aCO2	0.42	Last
6621	4	2017	11.155	11.903	111.277	eCO2	0.37	First
6621	4	2022	14.598	15.353	185.139	eCO2	0.38	Last
6632	4	2018	11.49	12.213	117.14	eCO2	0.36	First
6632	4	2022	11.248	11.977	112.657	eCO2	0.36	Last
6382	5	2017	15.03	15.733	194.419	aCO2	0.35	First
6382	5	2022	12.573	13.28	138.511	aCO2	0.35	Last
6406	5	2017	15.795	16.715	219.431	aCO2	0.46	First
6406	5	2022	16.747	17.658	244.9	aCO2	0.46	Last
3755	6	2017	11.74	12.459	121.922	eCO2	0.36	First
3755	6	2022	11.232	11.957	112.284	eCO2	0.36	Last
5846	6	2017	15.315	16.244	207.253	eCO2	0.46	First
5846	6	2022	16.083	17.028	227.73	eCO2	0.47	Last
6021	7	2017	13.3	14.134	156.898	Ghost	0.42	First
6021	7	2022	14.635	15.477	188.123	Ghost	0.42	Last
6027	7	2017	14.42	15.073	178.428	Ghost	0.33	First
6027	7	2022	11.568	12.238	117.629	Ghost	0.33	Last
3634	8	2017	13.195	14.051	155.067	Ghost	0.43	First
3634	8	2022	11.39	12.255	117.949	Ghost	0.43	Last
3642	8	2017	10.675	11.222	98.916	Ghost	0.27	First
3642	8	2022	9.802	10.371	84.483	Ghost	0.28	Last
7331	9	2017	16.875	17.671	245.246	Ghost	0.40	First
7331	9	2022	16.785	17.599	243.246	Ghost	0.41	Last
7476	9	2017	9.685	10.373	84.501	Ghost	0.34	First
7476	9	2022	10.967	11.668	106.918	Ghost	0.35	Last

55 Table S6: Table of canopy spread v. bark radius and canopy spread diameter data for oak. Two separate repeat measures (First at installation year, Last early 2022) are listed. Bark radius is for the year of measurement.

Section 3.3



60 **Figure S6: (a) Ghost and Infrastructure TWU (litres d⁻¹) boxplots years 2017-2019. Boxplots 2018, 2019, show mean daylight daily tree water usage (\overline{TWU} , litres d⁻¹) combined by treatment for each treatment month April to October. (b) \overline{TWU}_n (litres d⁻¹ mm⁻¹), i.e. TWU normalised by tree radius (mm) at stem probe insertion height. Numbers of trees with both sap probeset installations functioning differs by month and year from July 2017 (2 trees) until Oct 2019 (18 trees). Mean values, calculated from the entire range of data, are shown as spots (pink).**



65 **Figure S7: Comparison of monthly water usage data for all trees with individual tree ids., showing (a) sap flux (litres s^{-1}) 95%iles (2017–2018) (b) sap flux (litres s^{-1}) 95%iles (2019–2021), and (c) TWU_n (litres $day^{-1} mm^{-1}$) 95%iles (2019–2021. Panels across seasons 3 to 5 of treatment) with Y axis commencing at 0.5 litres $day^{-1} mm^{-1}$. (a) and (b) colours correspond to individual trees. (a) years 2017 and 2018, scaled to show a maximum of 0.03 $l s^{-1}$. (b) years 2019, 2020 and 2021, scaled to show a maximum of 0.25 $l s^{-1}$. (c) symbols are individual trees, colours are treatment type.**

Note on Outliers

65 Outliers (Figures S7) influence tree water usage even when normalised for tree size. Peak variations of TWU (litres d^{-1}) and TWU_n (litres $d^{-1} mm^{-1}$) (main document Fig. 5 and Fig. S5(c)), influenced by outliers, can be extreme for the infrastructure arrays. We cannot conclusively deduce inter-treatment comparisons without outlier temporal synchronicity or consistent removal prior to analysis. This check has now been done for TWU_n data across the season (2019–2021) as part of the analysis of variance. It is interesting to note that in 2021 for example, outliers appear to have been more prevalent in the aCO_2 trees in June, July and August, and more prevalent in the eCO_2 trees in June, July and September, with outliers in *Ghost* trees always being less frequent and smaller than for aCO_2 trees. This may imply a delayed effect of infrastructure present in eCO_2 compared to

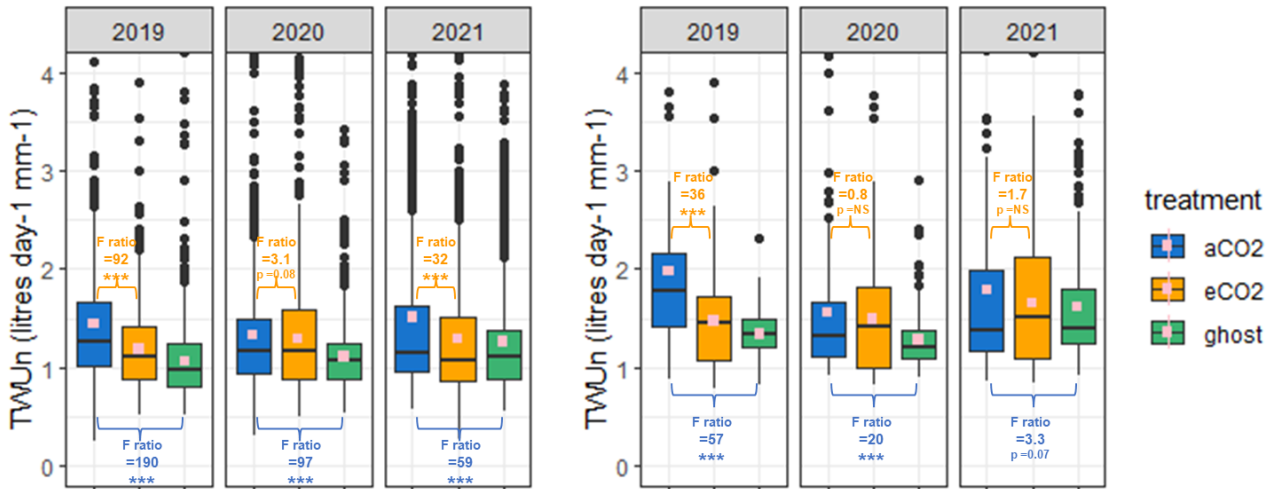
75

aCO₂, so inter-monthly comparisons may be distorted when compared to each control treatment, or between controls.

Section 3.4

(a) Treatment season

(b) July



80 Figure S 8: Treatment comparison of TWU_n . For years 2019–2021 the TWU_n (litres $d^{-1} mm^{-1}$) data is shown for the three
 85 treatment types. (a) The season data April–October is combined for each year. (b) July for each year is shown. The
 distributions are shown as box and whisker plots showing median and interquartile range (IQR, 25%ile to 75%ile)
 with whiskers calculated as 1.5 x IQR from the hinge and points for outliers. Mean values, calculated from the entire
 range of data i.e. season (a) or July (b) are shown as spots (pink). p-values and F ratios are indicated in orange
 (hypothesis 1, Table 4) for eCO_2 : aCO_2 one-way ANOVA model and blue (hypothesis 2, Table 5) for aCO_2 : $Ghost$ one-
 way ANOVA model. Values for both treatment season (a) and July mean (b) TWU_n in each year are given. Tables also
 give % differences of both treatment season and July mean TWU_n .

	2019 p value	2019 F ratio	2019 %	2020 p value	2020 F ratio	2020 %	2021 p value	2021 F ratio	2021 %
Season	< 0.001	91.90	-19%	p>0.05, actual value 0.079	3.09	-3%	<0.001	32.27	-13.9%
July only	< 0.001	35.61	-26%	p>0.05, actual value 0.37	0.80	-4.5%	p>0.05, actual value 0.19	1.71	-7.3%

90 Table S 7: Hypothesis 1 CO₂ effects. One-way ANOVA p-value, F ratio, and % difference summary for mean eCO_2
 TWU_n , compared with mean aCO_2 TWU_n , in years 2019–2021. Mean values are compared, calculated from the entire
 range of data for season data April–October (Fig. S8(a)) and July (Fig. S8b), for each year as shown. Bold typeface
 indicates p-value <0.05.

	2019 p value	2019 F ratio	2019 %	2020 p value	2020 F ratio	2020 %	2021 p value	2021 F ratio	2021 %
Season	< 0.001	187.38	+37%	< 0.001	96.66	+20%	<0.001	58.81	+20%
July only	< 0.001	57.35	+48%	< 0.001	19.95	+22%	p>0.05, actual value 0.071	3.29	+9.9%

95 Table S 8: Hypothesis 2 infrastructure effects. One way ANOVA p-value, F ratio, and % difference summary for aCO_2
 compared with $Ghost$ TWU_n in years 2019–2021. Mean values are compared, calculated from the entire range of data
 for season data April–October (Fig. S8(a)) and July (Fig. S8(b)) for each year as shown. Bold typeface indicates p-
 value <0.05.

ANOVA model notes

100 Hypothesis 1 concerning the effect of CO₂ was tested by one-way ANOVA between $eCO_2 \overline{TWU_n}$ compared with
 $aCO_2 \overline{TWU_n}$ (Table S7, Fig. S8).

In 2019 and 2021 seasons, the ANOVA suggested a highly significant ($p < 0.001$), -19% to -13.9%, reduction in $eCO_2 \overline{TWU}_n$ compared with $aCO_2 \overline{TWU}_n$ (Fig. S8 blue-yellow comparisons, Table S7). In 2020, the 3% reduction was marginally significant ($p = 0.08$) for $eCO_2 \overline{TWU}_n$ vs. $aCO_2 \overline{TWU}_n$. For July-only results, the ANOVA suggested a highly significant ($p < 0.001$) -26% reduction in $eCO_2 \overline{TWU}_n$ compared with $aCO_2 \overline{TWU}_n$ in July 2019, whilst comparisons for July 2020 and July 2021 showed no significant differences (Fig. S8 blue-yellow comparisons, Table S7).

Hypothesis 2 concerning the effect of infrastructure is tested by one-way ANOVA between mean values of $aCO_2 \overline{TWU}_h$ compared with $Ghost \overline{TWU}_h$ (Table S8, Fig. S8 blue-green comparisons). For all 2019, 2020 and 2021 seasons, the ANOVA suggested a highly significant ($p < 0.001$) 37% to 20% increase in $aCO_2 \overline{TWU}_n$ compared with $Ghost \overline{TWU}_n$ (Fig. S8, Table S8). For July-only \overline{TWU}_n , the ANOVA suggested a highly significant ($p < 0.001$) 48% to 22% increase in aCO_2 compared with $Ghost \overline{TWU}_n$ for July 2019 and July 2020 (Fig. S8, Table S8). For July 2021, a marginal 10% effect for $aCO_2 \overline{TWU}_n$ vs. $Ghost \overline{TWU}_n$ was found ($p = 0.07$).

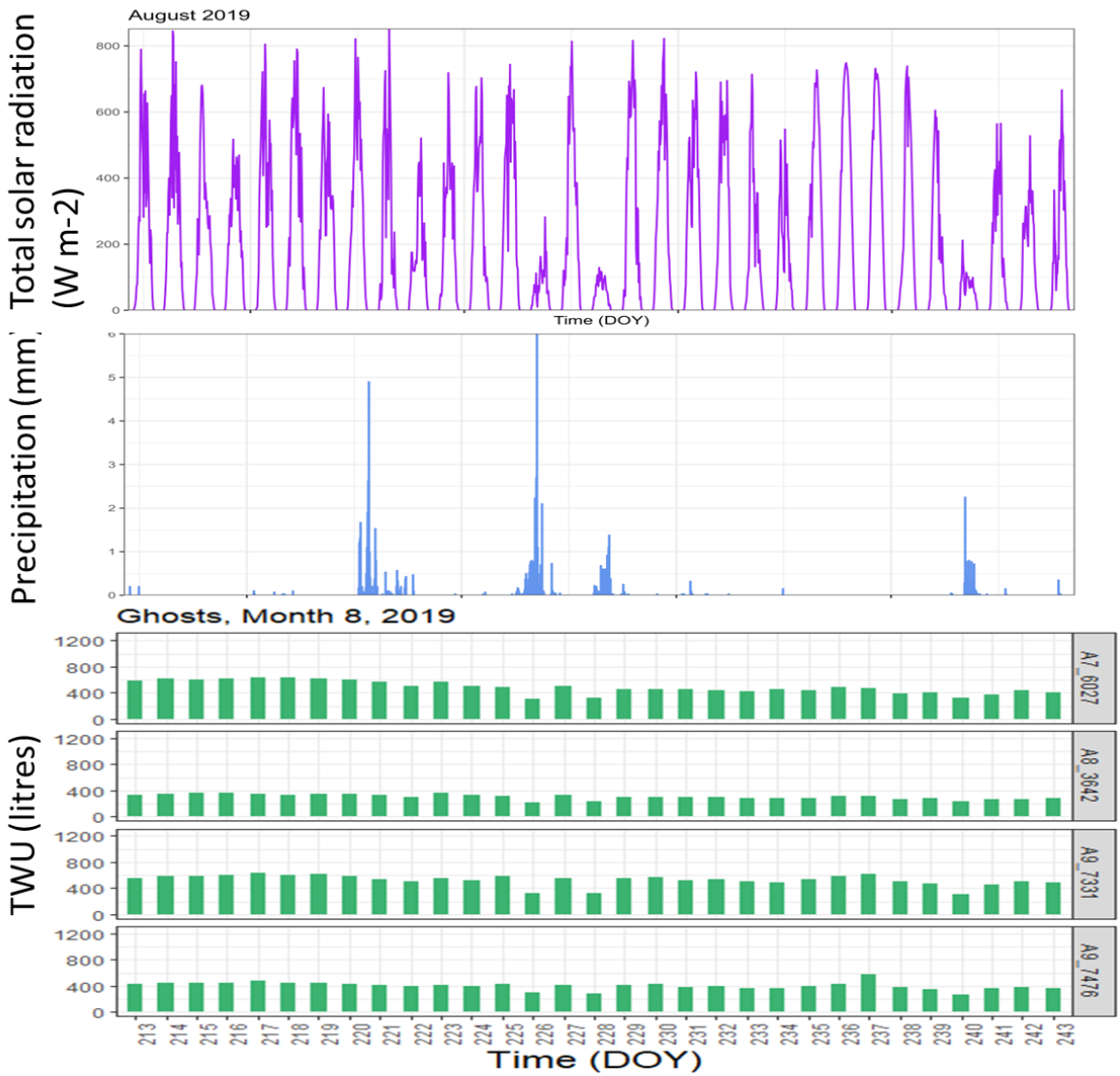


Figure S9: Example *TWU* (litres d⁻¹) per DOY v. solar radiation and precipitation for August 2019. Note if precipitation is nocturnal, then it does not influence *TWU* directly.

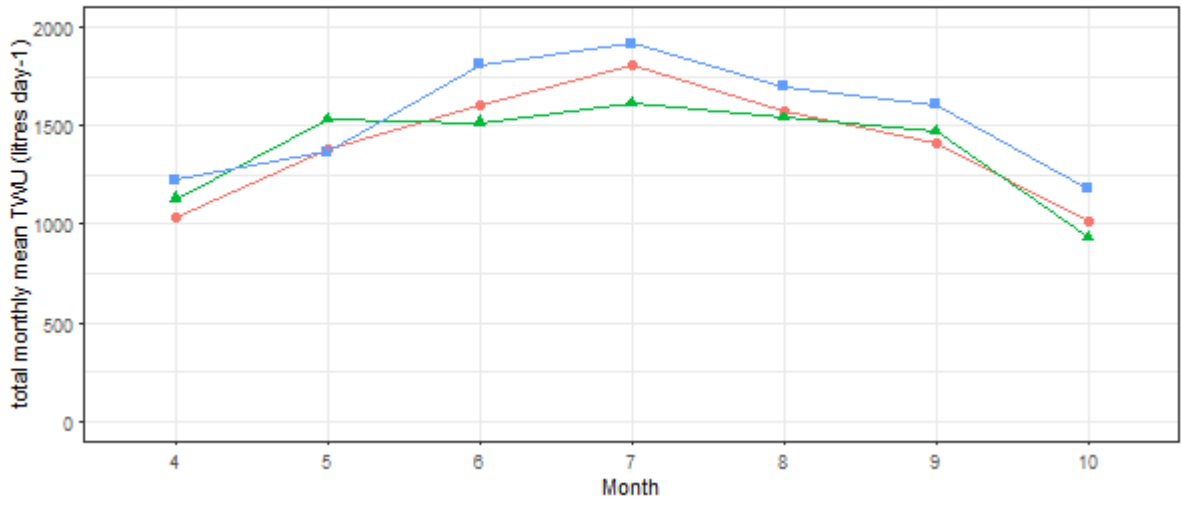
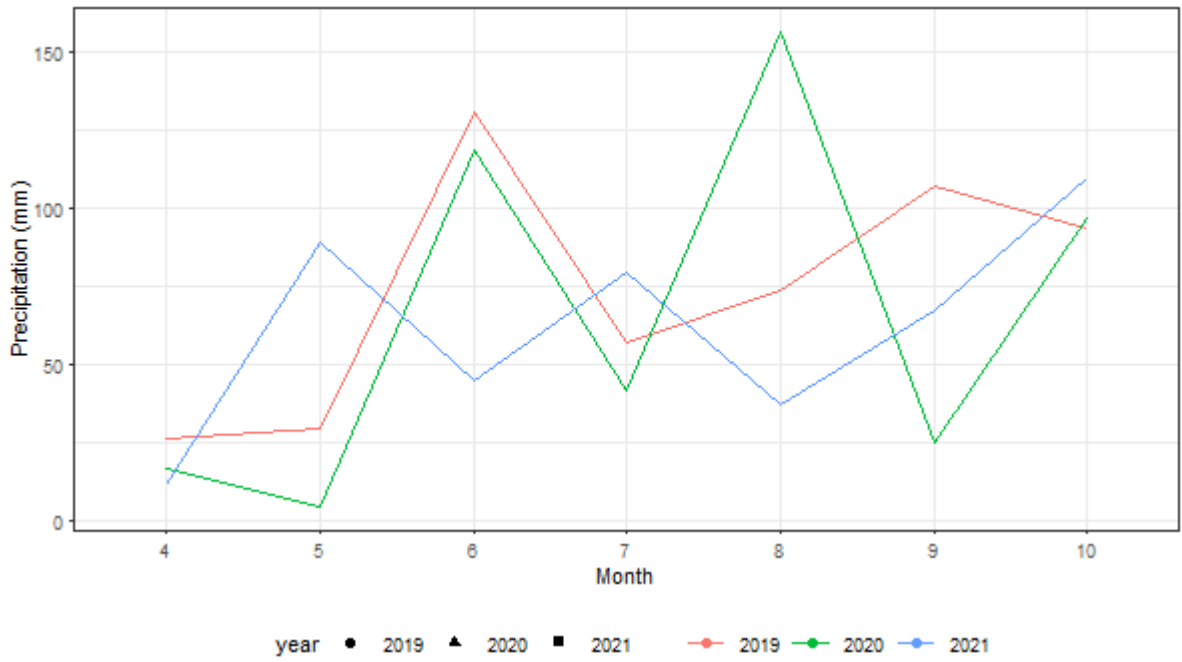


Figure S10: Monthly precipitation (mm) versus monthly mean TWU (\overline{TWU} , litres d-1) for treatment season months in years 2019 -2021.

Levene's test and model_CO2 for eCO₂ compared with aCO₂: Table S9.

All Levene tests (mean and median) for seasonal data 2019 and 2021 are significant; also for July data in 2019. This implies heterogeneity of variances of the data. For 2020 season and July 2020 and 2021 the test is not significant meaning ANOVA model can be validated for parametric assumptions.

	2019	2019	2020	2020	2021	2021
Season	F(1, 2065) =	Pr(>F)	F(1, 2491) =	Pr(>F)	F(1,2167) =	Pr(>F)
mean	58.697	***	0.474	0.4912	40.141	***
median	39.179	***	0.0332	0.8555	13.69	***
July	F(1, 300) =	Pr(>F)	F(1, 367) =	Pr(>F)	F(1,304) =	Pr(>F)
mean	11.07	***	0.7235	0.3956	5.3071	0.02191 *
median	7.7959	**	0.003	0.9563	0.8713	0.3513

125 **Table S9: Levene's test mean and median CO₂ effect eCO₂ compared with aCO₂. Bold results (2020 and 2021) are non-significant exhibiting homogeneity of variances.**

Levene's test and model_inf for aCO₂ compared with Ghost: Table S10

All tests both for seasonal and for July data 2019, 2020 2021 are significant demonstrating the heterogeneity of variances of the data.

	2019	2019	2020	2020	2021	2021
Season	F(1, 1962) =	Pr(>F)	F(1, 2491) =	Pr(>F)	F(1, 2438) =	Pr(>F)
mean	96.972	***	112.05	***	130.93	***
median	70.25	***	78.943	***	53.131	***
July	F(1, 277) =	Pr(>F)	F(1, 367) =	Pr(>F)	F(1, 338) =	Pr(>F)
mean	35.15	***	35.026	***	19.54	***
median	26.984	***	19.905	***	7.989	**

130 **Table S10: Levene's test mean and median infrastructure effect aCO₂ compared with Ghost. No results are non-significant so homogeneity of variances is not proven.**

Notes on Levene tests.

Despite limitations to the comparison of mean daily values, given the non-linear nature of the *TWU* data exhibiting variable outliers, the one-way ANOVA models using *TWU_n* provide a good initial indication of treatment comparisons when sufficient periods of time (here whole season or whole of July) of continuous data are compared between treatments, in line with the Central Limit Theorem.

Section 2.5 and 3.4

Annual mean solar radiation and air temp from FACE monitoring (top of 6 infrastructure arrays)
2017 – 2018 2019-2020 2021-

Extracted from 30min FACE
data files.
Jan 2022 & Jun 2022

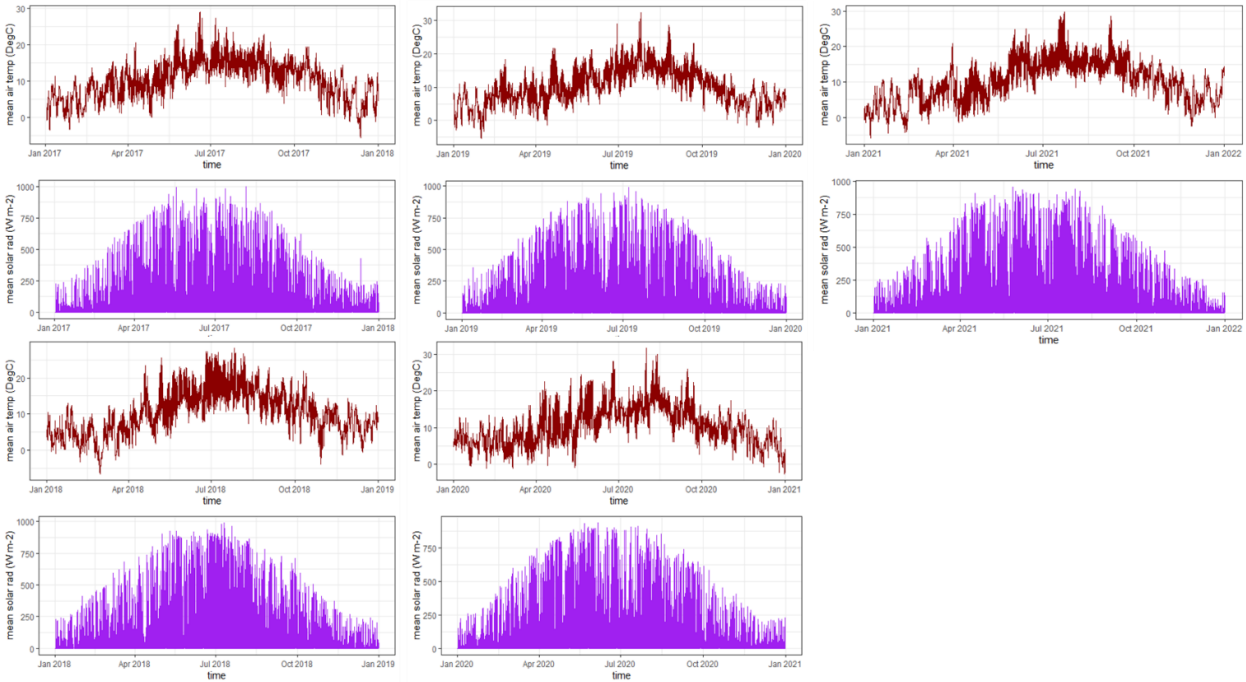


Figure S11: Annual mean solar radiation ($W\ m^{-2}$) and air temp (degrees C) for 2017 to 2021 from FACE monitoring (top of six infrastructure arrays).

Season	Tree numbers removed	No. of tree data used	Max number of days in season	Total treedays modelled
CO₂ model (eCO₂: aCO₂)				
2019	A1_8467 and A3_8351 low data	10	214	2047
2020	none	12	214	2493
2021	A4_6632 (failed) A5_6382 low data (98 days)	10	214	2071
Infrastructure model (aCO₂: Ghost)				
2019	A3_8351, A7_6021 & A8_3634 low data	9	214	1841
2020	none	12	214	2493
2021	A5_6382 low data	11	214	2342

Table S 11: Data used in glmm models for hypothesis 1 and hypothesis 2

	2019	2020	2021
σ^2	0.07	0.08	0.11
τ_{00} DOY	0.03	0.03	0.04
τ_{00} treelabel	0.01	0.01	0.02
ICC	0.37	0.35	0.34
Marginal R ² / Conditional R ²	0.041 / 0.399	0.003 / 0.348	0.046 / 0.371

Table S 12: Detailed statistics from the glmm model to test hypothesis 1

	2019	2020	2021
σ^2	0.08	0.06	0.08
τ_{00} DOY	0.03	0.03	0.03
τ_{00} treelabel	0.02	0.01	0.01
ICC	0.37	0.35	0.34
Marginal R ² / Conditional R ²	0.097 / 0.433	0.061 / 0.390	0.029 / 0.355

Table S 13: Detailed statistics from the glmm model to test hypothesis 2

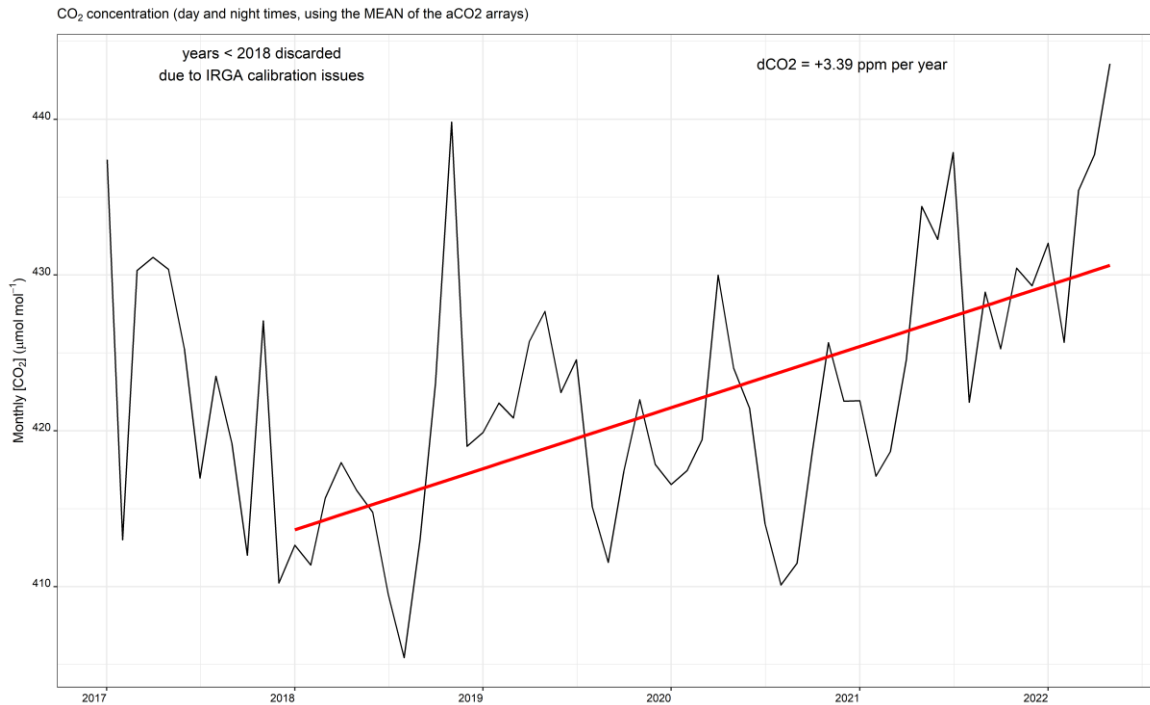
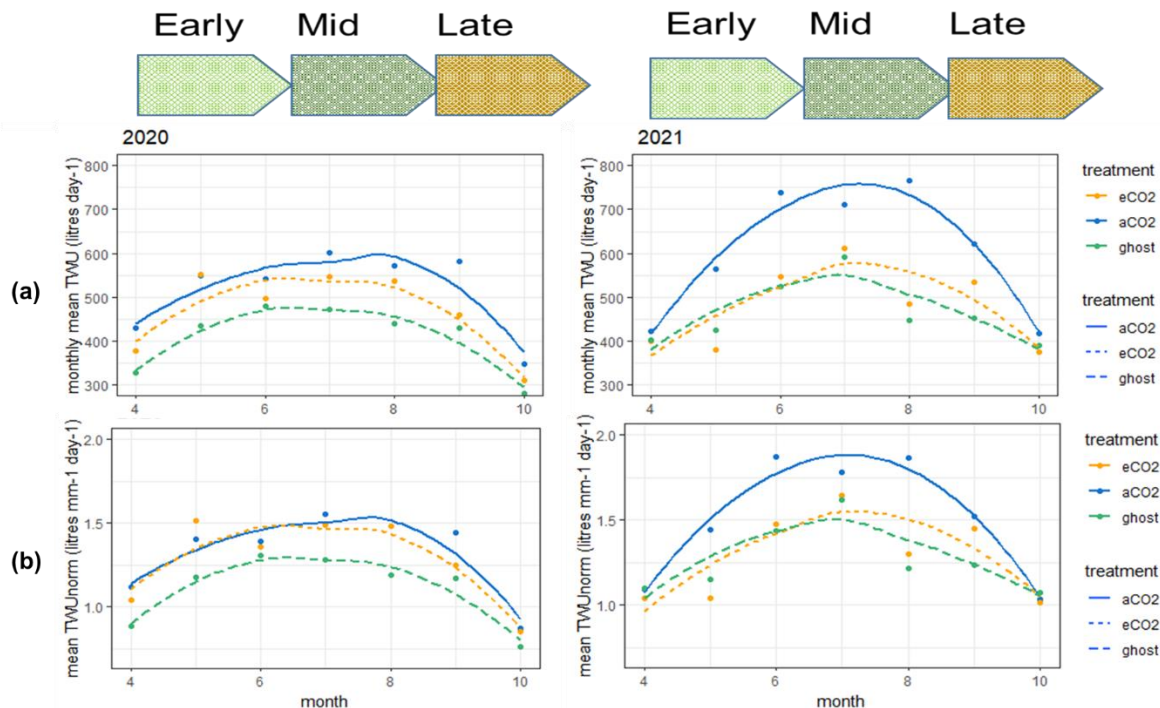


Figure S12: Ambient CO₂ concentration at BIFoR FACE experiment during years 2018 to 2021 (day and night times, using the mean of the aCO₂ arrays). The red line represents the slope of the increase over that period. Note pre-2018 data are calibrated differently.

Example visualisation (referenced Section 2.9).



150 Figure S13: Seasonal changes in water usage (a) \overline{TWU} , (litres d⁻¹ month⁻¹), grouped by treatment (up to 6 trees), for each treatment month in 2020 & 2021. (b) \overline{TWU}_n , (litres d⁻¹ mm⁻¹ month⁻¹), grouped by treatment (up to 6 trees), for each treatment month in 2020 & 2021. The lines use method = 'loess' and formula 'y ~ x'.

Note on monthly mean TWU and TWU_n (\overline{TWU} and \overline{TWU}_n).

155 Figure S13 indicates \overline{TWU} (litres d⁻¹ month⁻¹) and \overline{TWU}_n (litres d⁻¹ mm⁻¹ month⁻¹) for each treatment season month in 2020 and 2021 to more clearly visualise those data. The seasonality of \overline{TWU} and \overline{TWU}_n at senescence is different in the two years.

160 Supplement Appendix S-A.

Environmental and soil parameters.

For plants, incident precipitation affects their function in several ways during the leaf-on season. Firstly, water droplets fall on the leaves which combined with lack of sun can prevent full photosynthesis. The canopy water mostly evaporates or may drip to ground. Secondly throughfall (P_{fs} , mm) reaching ground level may either: runoff
165 the surface being lost to the soil, infiltrate increasing soil moisture content (providing some necessary support for root rehydration and plant water intake) or evaporate. Lastly, the soil water percolates through the saturated soil layers to replenish the water table.

Tor-ngen et al. (2014) found no significant interaction effects between sap flux derived canopy conductance eCO_2 changes and soil moisture (using relative extractable water).

170 Seasonal weather

Local reference precipitation (P_r , mm) for the period of interest (November 2015 to December 2021) in both the meteorological year and the tree hydraulic year averages to approximately 748 mm yr⁻¹ (Table S14). All years are reported, for completeness and to provide a broader context for the years for which we report sapflux data. We focus on hydraulic Years 3–5 (2019–2021) to interpret the rank ordering of our results for eCO_2 treatment effect
175 on TWU (Hypothesis 1) in the light of interannual climate variability. From Table S7, above, the magnitudes of both the seasonal and July-only eCO_2 treatment effects are ranked (lowest to highest) in the order 2020, 2021, 2019.

Effects of precipitation on deciduous tree water usage

Table S14 reports Early leaf-on (May to June), Mid leaf-on (July to August) and Late leaf-on (September to
180 October) variability in P_r ; the pattern is shown qualitatively in Figure S14. Dormant (November to February) and pre-budburst (March to April) P_r are also shown, with the preceding dormant season typically providing about 50% of the precipitation in the plant hydraulic year. Replenishment of perched water table and ground water reservoir levels, influences utilisation by old growth oak (Süßel and Brüggemann, 2021) during summer drought. The wettest and driest years and leaf-on seasons in respect of the tree hydraulic year are also marked (Table
185 S14). Year 2 of the study (2017–2018) was the driest hydraulic year (HY) overall despite a very wet pre-budburst. During the growing season P_r averages 499 mm (Table S14). HY 5 (2020–2021) was the wettest of these three years overall but exhibited less than average growing season precipitation. HY 3 (2018–2019) had the wettest growing season.

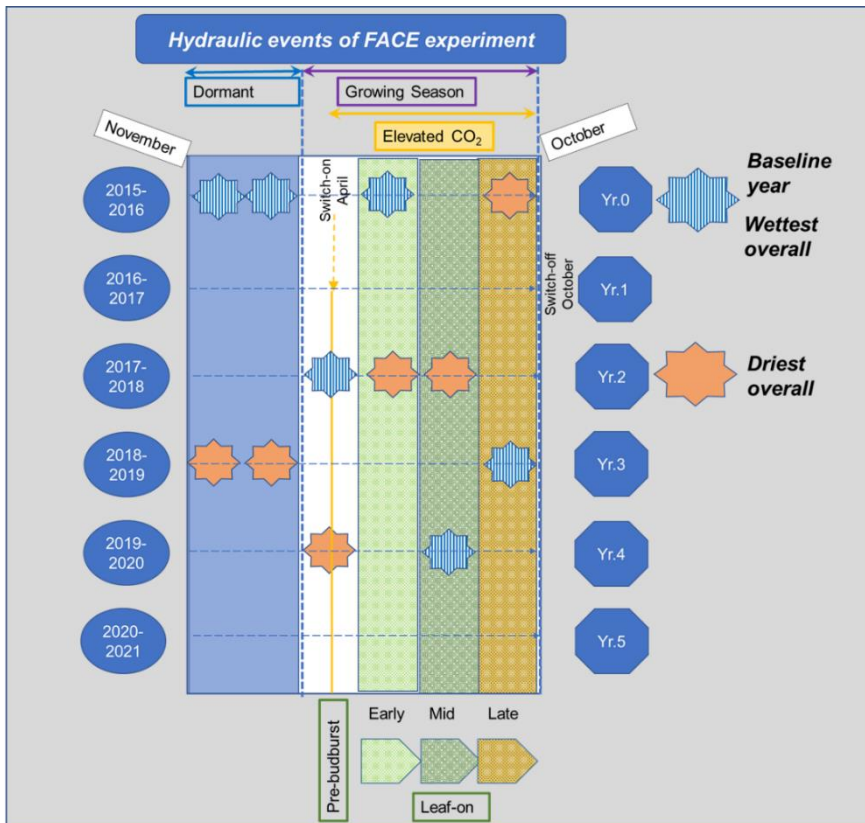
The rank order of growing season TWU_n follows that of growing-season precipitation: i.e. 2021, 2020, 2019
190 (lowest to highest), which indicates the control of TWU_n by water supply, but the association is indicative at best. The rank order of eCO_2 treatment effects follows that of sub-seasonal precipitation, both May-June and Sep-Oct: i.e., 2020, 2021, 2019.

For the treatment season, monthly throughfall (P_f , mm), i.e. average precipitation received at soil level, and monthly interception (P_i , mm), are shown in Fig. S15, across the five treatment years. Reference precipitation April–October (100%) minus treatment season throughfall (P_{fs} , %), by month and treatment season, gives interception percentage (P_{is} , %). Treatment season throughfall averages 59% per month. Annual throughfall averages 64% across the five years presented.

Throughfall percentages are influenced by changes to canopy cover and affected by herbivory defoliation (recorded in May 2018 and 2019). Another driver of high throughfall is heavy rain, which reduces interception. The rank order of interception minima (excluding early leaf-on and defoliation periods) is 6% July 2019, 7% in August 2020 and 11% in October 2019. Throughfall has not yet been quantitatively associated with TWU or \overline{TWU} due to the complexity of mixed effects in respect of other environmental influences (e.g. solar radiation, Figs. S9 & S11, and monthly precipitation versus \overline{TWU} , Fig. S10). To fully assess these interception factors LAI data is required which was not available for all years of this study. We present interception and throughfall (Fig. S15) here to inform future analyses through modelling.

FACE Treatment season label	Treatment	Reference Precipitation P_r (mm)						Mean
		2016	2017	2018	2019	2020	2021	
Year		2016	2017	2018	2019	2020	2021	Mean
Annual (Jan-Dec)		871.3	713.2	625.9	758.9	741.3	780.7	748.6
Tree hydraulic year		2015-6	2016-7	2017-8	2018-9	2019-20	2020-21	
Annual (Nov-Oct)		<u>913.5</u>	720.9	<u>649.2</u>	718.2	721.4	759.3	747.1
% anomaly to mean 2015-2021		22.3	-3.5	-13.1	-3.9	-3.4	1.6	0.0
November – Feb	Dormant	<u>296.6</u>	273.4	225.7	<u>151.9</u>	244.3	296.3	248.0
March – April	Pre-budburst	153.6	68.3	<u>178.2</u>	74.4	<u>34.2</u>	35.7	90.7
May – June	Early leaf-on	<u>202.3</u>	106.2	<u>61.5</u>	160.3	123.0	134.0	131.2
July – August	Mid leaf-on	153.9	157.4	<u>64.5</u>	130.8	<u>198.4</u>	116.5	136.9
September – October	Late leaf-on	<u>107.1</u>	115.6	119.4	<u>200.8</u>	121.6	176.8	140.2
March – Oct	Growing	<u>616.9</u>	447.4	<u>423.5</u>	566.4	477.1	463.0	499.1
eCO ₂ effect (%)		<u>n/a</u>	n/a	<u>n/a</u>	-19	-3	-14	

Table S 14: Precipitation totals and percentage deviations from mean across the seasons and years of interest. 2016 (2015/2016) included as a pre-treatment year. Calendar years are shown in rows 1-2; hydraulic year is used in the remainder of the table. Underline is maximum and underline is minimum of the years. Where data is not available it is marked “n/a”.



210 **Figure S 14:** Hydraulic events during period November 2015 to October 2021, baseline Year 0 and Years 1 to 5 of the FACE experiment. Year 2 (2017–2018) was the driest hydraulic year overall and year 3 (2018–2019) was the wettest treatment growing season (Table S14) including a very wet late leaf-on season.



Figure S 15: Local monthly precipitation, shown as stacked throughfall (P_f mm) and interception (P_i mm), at BIFoR FACE for treatment seasons 2017 to 2021. Percentage throughfall is indicated above each combined bar.

Shallow soil moisture response to treatment season precipitation

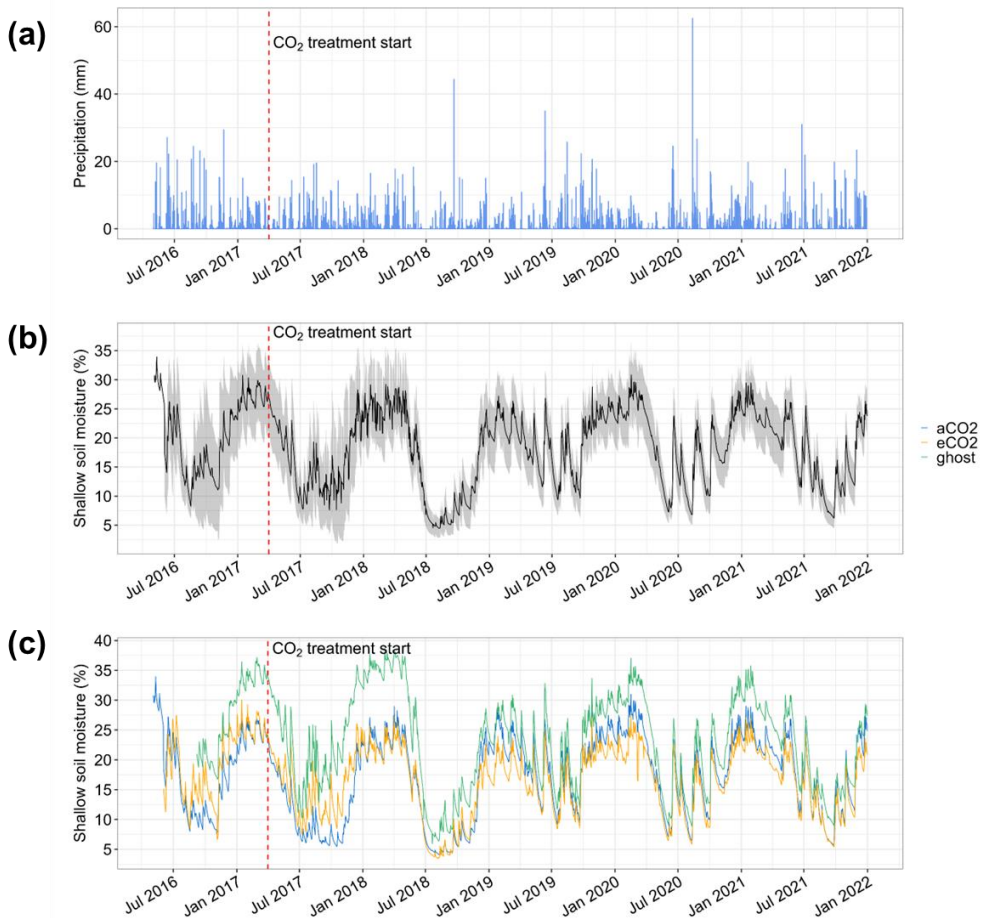


Figure S 16: Years 2016–2021 (a) daily precipitation (b) daily shallow soil moisture + sd averaged across all treatment arrays (c) daily mean shallow soil moisture by treatment. Extended from MacKenzie et al., 2021.

220 Throughfall during the treatment season (Fig. S15) directly affects Volumetric Water Content (VWC) and may therefore influence *TWU* from budburst to senescence. The extent of shallow (0 to 20cm depth) soil moisture depletion during drought and its effects on water usage by BIFoR FACE control (*aCO₂* and *Ghost*) oaks has been reported by Rabbai et al. (2023). Shallow soil moisture availability decreases progressively across the leaf-on season even in wet summers (MacKenzie et al., 2021 and Fig. S16).

225 Comparing Figs. 5 (main text) and S16, the opposite seasonalities of *TWU* and VWC are evident with autumn–winter dormant season providing VWC recharge. Tree water usage drives the leaf-on seasonal reduction in VWC, although the leaf season VWC cycle is strongly modulated by precipitation (e.g., Fig. S16, summer 2020). On shorter, sub-seasonal and daily timescales, the relationship between *TWU* and VWC is not expected to be simple. We defer a full account of sub-seasonal *TWU* v. VWC relations to future work, but note here in passing

230 that, for example during the most pronounced continuous dry period of the observation period (June to July 2018, Fig. S16), there appears to be no inter-year difference in median *Ghost* tree diurnal sap flux (Fig. 2(a)), 95%ile sap flux (Fig. S5), or median *TWU* ((Fig. S6) in all *Ghost* trees.

References

- 235 Čermak, J., KUČERA, J., and ŠTĚPÁNKOVÁ, M.: Water consumption of full-grown oak (*Quereus robur* L.) in a floodplain forest after the cessation of flooding, <https://doi.org/10.1016/b978-0-444-98756-3.50034-4>, 1991.
- David, T. S., Pinto, C. A., Nadezhdina, N., Kurz-Besson, C., Henriques, M. O., Quilhó, T., Cermak, J., Chaves, M. M., Pereira, J. S., and David, J. S.: Root functioning, tree water use and hydraulic redistribution in *Quercus suber* trees: A modeling approach based on root sap flow, *For. Ecol. Manage.*, 307, 136–146, <https://doi.org/10.1016/j.foreco.2013.07.012>, 2013.
- 240 Hemery, G. E., Savill, P. S., and Pryor, S. N.: Applications of the crown diameter–stem diameter relationship for different species of broadleaved trees, *For. Ecol. Manage.*, 215, 285–294, <https://doi.org/https://doi.org/10.1016/j.foreco.2005.05.016>, 2005.
- Rossi, S., Anfodillo, T., and Menardi, R.: Trephor: A New Tool for Sampling Microcores from tree stems, *IAWA J.*, 245 27, 89–97, <https://doi.org/https://doi.org/10.1163/22941932-90000139>, n.d.
- Sánchez-Pérez, J. M., Lucot, E., Bariac, T., and Trémolières, M.: Water uptake by trees in a riparian hardwood forest (Rhine floodplain, France), *Hydrol. Process.*, <https://doi.org/10.1002/hyp.6604>, 2008.
- Tatarinov, F. a, Kučera, J., and Cienciala, E.: The analysis of physical background of tree sap flow measurement based on thermal methods, *Meas. Sci. Technol.*, 16, 1157–1169, <https://doi.org/10.1088/0957-0233/16/5/016>, 250 2005.